Epidermal Iontophoresis: II. Application of the Ionic Mobility-Pore Model to the Transport of Local Anesthetics

Pamela M. Lai[1] and Michael S. Roberts[1,2]

Purpose. An in vitro study was carried out to determine the iontophoretic permeability of local anesthetics through human epidermis. The relationship between physicochemical structure and the permeability of these solutes was then examined using an ionic mobility-pore model developed to define quantitative relationships.

Methods. The iontophoretic permeability of both ester-type anesthetics (procaine, butacaine, tetracaine) and amide-type anesthetics (prilocaine, mepivacaine, lidocaine, bupivacaine, etidocaine, cinchocaine) were determined through excised human epidermis over 2 hrs using a constant d.c. current and Ag/AgCl electrodes. Individual ion mobilities were determined from conductivity measurements in aqueous solutions. Multiple stepwise regression was applied to interrelate the iontophoretic permeability of the solutes with their physical properties to examine the appropriateness of the ionic mobility-pore model and to determine the best predictor of iontophoretic permeability of the local anesthetics.

Results. The logarithm of the iontophoretic permeability coefficient (log $PC_{j,iont}$) for local anesthetics was directly related to the log ionic mobility and MW for the free volume form of the model when other conditions are held constant. Multiple linear regressions confirmed that log $PC_{j,iont}$ was best defined by ionic mobility (and its determinants: conductivity, pK_a and MW) and MW.

Conclusions. Our results suggest that of the properties studied, the best predictors of iontophoretic transport of local anesthetics are ionic mobility (or pK_a) and molecular size. These predictions are consistent with the ionic mobility pore model determined by the mobility of ions in the aqueous solution, the total current, epidermal permselectivity and other factors as defined by the model.

KEY WORDS: iontophoresis; local anesthetics; ionic mobility; pore; model.

INTRODUCTION

There have been several models derived to describe the movement of solutes during iontophoresis (1,2,3). We recently developed an ionic mobility—pore model to integrate solute size and solution composition as determinants of iontophoretic transport (4). The overall determinants described in the model were ion mobility, solute size, total current applied, presence of extraneous ions, epidermal permselectivity in the prediction of iontophoretic flux and interaction between the solute and organic components of the pore (4).

The purpose of the present study was to apply the ionic mobility-pore model developed earlier (4) to the iontophoresis of a group of similar solutes, the local anesthetics, and to

[1] Department of Medicine, University of Queensland, Princess Alexandra Hospital, Brisbane, Queensland 4102, Australia.
[2] To whom correspondence should be addressed. (e-mail: m.roberts@mailbox.uq.edu.au)

examine chemical properties such as conductivity, MW and pK_a as determinants of iontophoretic transport through human skin.

Theoretical Considerations

Previously, we have derived an equation for the overall iontophoretic transport of a solute j, $J_{j,iont,overall}$ through skin (4):

$$J_{j,joint,overall} =$$

$$\left(\frac{2\mu_j fi_j Fz_j I_T \Omega PRT_j}{(k_{s,d} + k_{s,r})[1 + fu_j\theta_{ju} + (1 - fu_j)\theta_{ji}]} \pm (1 - \sigma_j)v_m \right) C_j \quad (1)$$

where μ_j is the mobility of the solute, fi_j and fu_j are the fraction of the solute ionized and unionized, respectively, F is Faraday's number, z_j is the charge, I_T is the total current density, Ω is the permselectivity term, $k_{s,d}$ and $k_{s,r}$ are the conductivity of the donor and receptor compartment, respectively, θ_{ju} is the interaction of the unionized solute with the pore walls, θ_{ji} is the interaction of the ionized solute with the pore walls, PRT_j is the pathway restriction term, σ_j is the reflection coefficient, v_m is the average velocity of convective flow and C_j is the concentration in solution. Equation 1 can also be expressed in terms of the overall iontophoretic permeability coefficient $PC_{j,iont,overall}$:

$$PC_{j,iont,overall} = \frac{J_{j,iont,overall}}{C_j} =$$

$$\frac{2\mu_j fi_j Fz_j I_T \Omega PRT_j}{(k_{s,d} + k_{s,r})[1 + fu_j\theta_{ju} + (1 - fu_j)\theta_{ji}]} \pm (1 - \sigma_j)v_m \quad (2)$$

When the solute in solution is completely ionized (when $fu_j = 0$), then equation 2 reduces to:

$$PC_{j,iont,overall} = \frac{2\mu_j Fz_j I_T \Omega PRT_j}{(k_{s,d} + k_{s,r})(1 + \theta_{ji})} \pm (1 - \sigma_j)v_m \quad (3)$$

We define the electromigration component in equation 3 as an iontophoretic permeability coefficient, $PC_{j,iont}$:

$$PC_{j,iont} = \frac{2\mu_j Fz_j I_T \Omega PRT_j}{(k_{s,d} + k_{s,r})(1 + \theta_{ji})} \quad (4)$$

Membrane Pathway Restriction of Iontophoretic Transport

In equations 1–4, two forms of the pathway restriction term are proposed (4), free volume and the pore-restriction. In the free volume form, the pathway restriction term (PRT_j^{FV}) is defined by the negative exponent of the ratio of the solute molecular volume MV to an effective average "cage" volume (V_{av}^i):

$$PRT_j^{FV} = exp\left(-\frac{MV}{V_{av}^i}\right) \quad (5)$$

When the electroosmotic component is negligible, and approximating MV by MW (5), expressing equation 5 in logarithmic form allows log $PC_{j,iont}$ (the electromigration component only) to be related to MW using the free volume form of PRT_j^{FV} (equation 6):

$$\log PC_{j,iont} = A + B \log \mu_j - C\,MW \qquad (6)$$

where A is a constant defined by total current, epidermal cation permselectivity and solution conductivity, B is a correction factor associated with the use of deionized distilled water and conductivity for estimation of mobility (value should theoretically be unity) and C is the reciprocal of the average molecular weight associated with iontophoretic transport through a "free volume" determined restricted pathway in the epidermis.

In the pore-restriction model, we defined PRT_j^{PR} terms of λ_j, the ratio of solute radius and pore radius, using either the approximate (equation 7), or the full expression (equation 8) (4):

$$PRT_j^{PR} = (1 - \lambda_j)^2(1 - 2.10\lambda_j + 2.09\lambda_j^3 - 0.95\lambda_j^5) \qquad (7)$$

for $0 \le \lambda_j < 0.4$, or

$$PRT_j^{PR} =$$

$$\frac{6\pi(1 - \lambda_j)^2}{3.18\pi^2(1 - \lambda_j)^{-5/2}\left[1 + \sum_{n=1}^{2} a_n(1 - \lambda_j)^n\right] + \sum_{n=0}^{4} a_{n+3}(\lambda_j)^n}$$

$$(8)$$

for $0 \le \lambda_j < 1$ where the coefficients are $a_1 = -1.22$, $a_2 = 1.53$, $a_3 = -22.51$, $a_4 = -5.61$, $a_5 = -0.34$, $a_6 = -1.22$ and $a_7 = 1.65$.

Convective Flow

Electroosmotic flow is defined as the bulk fluid flow which occurs when a potential difference is applied across a charged membrane (6). Whilst iontophoretic transport is dominant for small charged solutes, convective flow or electroosmotic flow is likely to be more significant for macromolecules (6).

The convective component of iontophoretic transport is also affected by pathway restriction, $(1 - \sigma)$. The electroosmotic reflection coefficient σ for a membrane is defined as the fraction of solute "reflected" or rejected by the membrane relative to water (7). For the free volume model, this pathway restriction term is also expressed as $\exp(-MV/V_{av}^\sigma)$. It is most likely that this V_{av}^σ would be shown to differ from that for iontophoresis V_{av}^i. The electroosmotic transport equations corresponding to equations 7 and 8 are (4,7):

$$1 - \sigma_j = (1 - \lambda_j)^2(2 - (1 - \lambda_j)^2)(1 - 0.667\lambda_j^2 - 0.163\lambda_j^3) \qquad (9)$$

for $0 \le \lambda_j < 0.4$ and

$$1 - \sigma_j$$

$$= \frac{(1 - \lambda_j)^2(2 - (1 - \lambda_j)^2)\left(3.18\pi^2(1 - \lambda_j)^{-5/2}\right.}{2\left(3.18\pi^2(1 - \lambda_j)^{-5/2}\right.}$$

$$\frac{\times \left[1 + \sum_{n=1}^{2} b_n(1 - \lambda_j)^n\right] + \sum_{n=0}^{4} b_{n+3}\lambda_j^n\Big)}{}$$

$$\left. \times \left[1 + \sum_{n=1}^{2} a_n(1 - \lambda_j)^n\right] + \sum_{n=0}^{4} a_{n+3}\lambda_j^n\right)} \qquad (10)$$

for $0 \le \lambda_j < 1$, where $b_1 = 0.12$, $b_2 = -0.04$, $b_3 = 4.02$, $b_4 = -3.97$, $b_5 = -1.92$, $b_6 = 4.39$, $b_7 = 5.01$.

Membrane and Solute Charge Effects on Transport

The charge of the solute and on the pore wall will affect the pathway restriction term. This influence can be modelled as a Debye layer l_D effect associated with charged surfaces on the effective radius of the moving charged solute and on the pore radius (8):

$$\lambda_j^* = \frac{r_j + l_D}{r_p - l_D} \qquad (11)$$

where λ_j^* is the effective solute to effective pore radius ratio and l_D is defined by (8):

$$l_D = \sqrt{\frac{\varepsilon kT}{8\pi z_s^2 e^2 N_A C_s}} \qquad (12)$$

where ε is the solution dielectric constant, k is Boltzmann's constant, T is the absolute temperature, z_s is the charge of the supporting solute, e is the fundamental charge of a proton, N_A is Avogadro's number, and C_s is the concentration of the supporting solute.

METHODS

Materials

Local anesthetics (lidocaine HCl, prilocaine HCl, mepivacaine HCl, cinchocaine HCl, tetracaine HCl, etidocaine HCl, bupivacaine HCl, butacaine, procaine HCl) were either purchased from Sigma Chemical Co. (Sydney), or a gift from Astra Sweden. HEPES (N-2-hydroxyethylpiperazine-N'-2-ethanesulphonic acid) buffer was purchased from Sigma Chemical Co.

Transport studies were carried out using 50 mM HEPES buffer as the donor solution. 10 mM of the appropriate local anesthetic and ^3H_2O was dissolved into the donor solution and pH adjusted to 4.5. Isotonic (based on SCE (9)) 20 mM HEPES buffer (pH 7.4 or 4.5) with 147 mM NaCl was used as the receptor solution. All buffers were prepared with deionized distilled water and adjusted to the appropriate pH with NaOH or HCl. Tritiated water was included to estimate water flow.

Skin

Full-thickness human, female abdominal skin was obtained from abdominoplasty at the Wesley Hospital, Brisbane, Queensland with approval by the Hospital's Ethics Committee. The epidermis was separated from these skin samples by the method of Kligman and Christophers (10). Briefly, the full-thickness skin was placed in a 60°C water-bath for 1 min. The epidermal membrane, which includes the stratum corneum and part of the epidermis, was then peeled away from the underlying dermis, the thickness of the epidermal membrane being about 100 μm. The transparent sheet of the epidermal membrane was then washed with water, excess moisture was removed by leaving the skin exposed to air at room temperature, and stored at −20°C. Membranes were thawed prior to use by immersing in deionized distilled water at room temperature followed by equilibration in isotonic 20 mM HEPES buffer for 1 hour at 37°C.

The epidermal membranes were mounted between two glass half-cells with the stratum corneum facing the donor compartment. The surface area of epidermis exposed to the

solution was 0.95 cm². The diffusion cells were then firmly clamped and immersed in a water bath maintained at 37 ± 0.5°C by a constant temperature bath heating system. The half-cell volume was 1.0 ml and both compartments were stirred with Teflon coated fleas using external magnets. Each experiment, carried at least in triplicate, used a fresh piece of epidermal membrane from one subject's abdominoplasty skin specimen each time. The experiments were carried out by anodal iontophoresis.

Anodal Iontophoresis

Constant current devices (custom made by the Department of Physical Sciences, Princess Alexandra Hospital) were used in the iontophoretic studies. Ag/AgCl electrodes were used with the anode was positioned in the donor compartment, and the cathode in the receptor compartment, 1 cm from the membrane. Current was passed at a density of 0.38 mA/cm².

The receptor volume (1.0 ml) was removed at designated times over the duration of the experiment (0, 15, 30, 45, 60 min) and immediately replaced with an equal volume of fresh receptor solution. At the completion of each study, samples were withdrawn from the donor solution. All studies were carried out at least in triplicate. Epidermal transport of these compounds under exactly the same conditions but without current, was also determined.

The specific conductance of the donor solutions was measured using a conductivity meter (Radiometer, Copenhagen, model CDM80). The intrinsic conductivity of solutes was measured in deionized distilled water at concentrations ranging from 1 mM to 10 mM to estimate the contribution of solute conductivities to the overall conductivity of the donor solution. Conductivity was measured by direct reading of the conductivity meter and given by:

$$k = \frac{d}{a} G \qquad (13)$$

where d is the distance between the electrodes and a is the area of the electrodes, d/a corresponds to the cell constant and G is the conductivity in reciprocal ohms. The units of specific conductance is S (siemens) per cm. The specific conductance of deionized distilled water was 0.50–0.75 μS/cm. The apparent mobility of each ion in solution μ_j is then calculated from k_{jw}, the solute concentration C_j used in the determination of the

conductivity, z_j (= 1 for all ions) and the Faraday number (9.648 × 10⁴ C/mol) using

$$\mu_j = \frac{k_{jw}}{FC_j z_j} \qquad (14)$$

HPLC of Local Anesthetics

HPLC analysis of the local anesthetics was performed using a Shimadzu LC-6AD pump, Perkin-Elmer LC90 Bio Spectrophotometric UV detector, Shimadzu SIL-6B autoinjector with SCL-6B system controller, delivering 50 μl sample injections directly onto a Waters C18 μ-Bondapak 3.9 × 300 mm column with data analysed using a Delta HPLC Data Acquisition integrator. The mobile phases consisted of mixtures of acetonitrile (ACN):phosphate 0.05M: TEA (triethylamine). The ratios of solvent in each mobile phase, the different wavelength used, retention times and detection limit for each of the local anesthetics are given in Table I. Samples were injected directly onto the column.

Data Analysis

Epidermal permeability rates were determined for each compound from plots of cumulative amounts detected in the receptor compartment as a function of time. The steady-state flux was calculated from the slope of the linear portion of each curve. Minitab statistical software (Minitab Inc., PA, USA) on a Macintosh LC475 computer was used to perform stepwise regressions. Nonlinear regressions were undertaken using MINIM 3.0.9 (11).
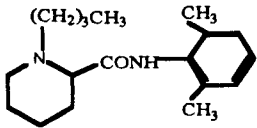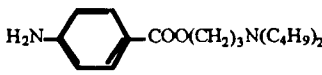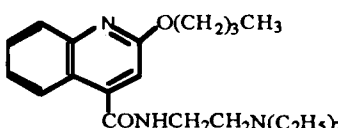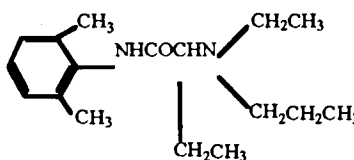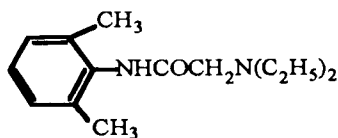
RESULTS AND DISCUSSION

The local anesthetics used in this study can essentially be categorized into two groups, the amide anesthetics (prilocaine, lidocaine, mepivacaine, etidocaine, bupivacaine and cinchocaine) and ester anesthetics (procaine, butacaine and tetracaine). The physicoch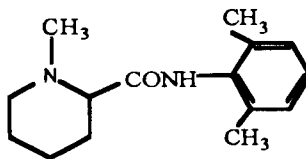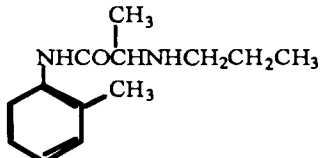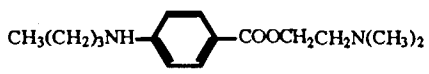emical properties of the local anesthetics, including molecular weight (MW) and pK_a, are given in Table II. The cumulative amount profile over time of the local anesthetics are shown in Fig. 1. The flux and iontophoretic permeability coefficient, $PC_{j,iont}$, of the local anesthetics with the donor solution at pH 4.5 and receptor at either pH 4.5 and 7.4 are given

Table I. HPLC Conditions for Local Anaesthetic Concentration Measurements

Local anesthetic	UV wavelength (nm)	Mobile phase ACN:phosphate 0.05M:TEA pH 4	Retention time (min)	Detection limit (μg/ml)	R^2 for calibration curve
Bupivacaine	260	35:65:1	4.63	0.5	0.99
Butacaine	260	50:50:1	4.15	0.5	0.99
Cinchocaine	320	50:50:1	4.82	0.5	0.99
Etidocaine	260	35:65:1	5.20	0.5	0.99
Lidocaine	260	20:80:1	6.90	0.5	0.99
Mepivacaine	260	20:80:1	6.84	0.5	0.99
Prilocaine	260	20:80:1	7.61	0.5	0.99
Procaine	286	20:80:1	4.66	0.5	0.99
Tetracaine	304	50:50:1	3.95	0.5	0.99

Table II. Physicochemical Properties of the Local Anesthetics

Local anesthetic		Type	MW	Intrinsic conductivity at pH 4.5 (μS/cm)	Log P^a	pKa^b
Bupivacaine	(CH₂)₃CH₃ / N / CONH / CH₃ / CH₃	amide	288.4	740	3.41	8.1
Butacaine	H₂N—⟨ ⟩—COO(CH₂)₃N(C₄H₉)₂	ester	306.4	1060	5.00*	9.0^c
Cinchocaine	N / O(CH₂)₃CH₃ / CONHCH₂CH₂N(C₂H₅)₂	amide	343.4	818	4.40	8.9
Etidocaine	CH₃ / NHCOCHN / CH₂CH₃ / CH₃ / CH₂CH₂CH₃ / CH₂CH₃	amide	276.4	780	3.69	7.7
Lidocaine	CH₃ / NHCOCH₂N(C₂H₅)₂ / CH₃	amide	234.3	773	2.26	7.9
Mepivacaine	CH₃ / N / CONH / CH₃ / CH₃	amide	246.3	770	1.95	7.7
Prilocaine	CH₃ / NHCOCHNHCH₂CH₂CH₃ / CH₃	amide	220.3	843	2.11	7.9
Procaine	H₂N—⟨ ⟩—COOCH₂CH₂N(CH₂CH₃)₂	ester	236.3	1143	1.92	9.0
Tetracaine	CH₃(CH₂)₃NH—⟨ ⟩—COOCH₂CH₂N(CH₃)₂	ester	264.3	900	3.73	8.4

Notes: Conductivity is measured in μSiemens/cm, at pH 4.5. Solution is 10 mM LA in d.d. H₂O at 25°C.
^{a} Log P values are taken from ClogP (Biobyte, Claremont, CA) observed data. *Estimated from ClogP.
^{b} Data from ref. 29, unless otherwise indicated.
^{c} Data from ref. 30.

in Table III. Epidermal transport, with no iontophoretic current, showed negligible flux, that is, the concentration of local anesthetic in the receptor compartment, after 2 hrs, was below the limit of HPLC detection. Procaine, an ester anesthetic, had the highest iontophoretic flux, whilst cinchocaine, an amide anesthetic, was shown to have the lowest iontophoretic flux.

Iontophoretic Transport Analysis

Figure 2 shows the relationship between $PC_{j,iont}$ and solute ion mobility with MW. It is apparent that the $PC_{j,iont}$-MW relationship for the local anesthetics parallels the ionic mobility-MW in the donor solution and that MW is a determinant of
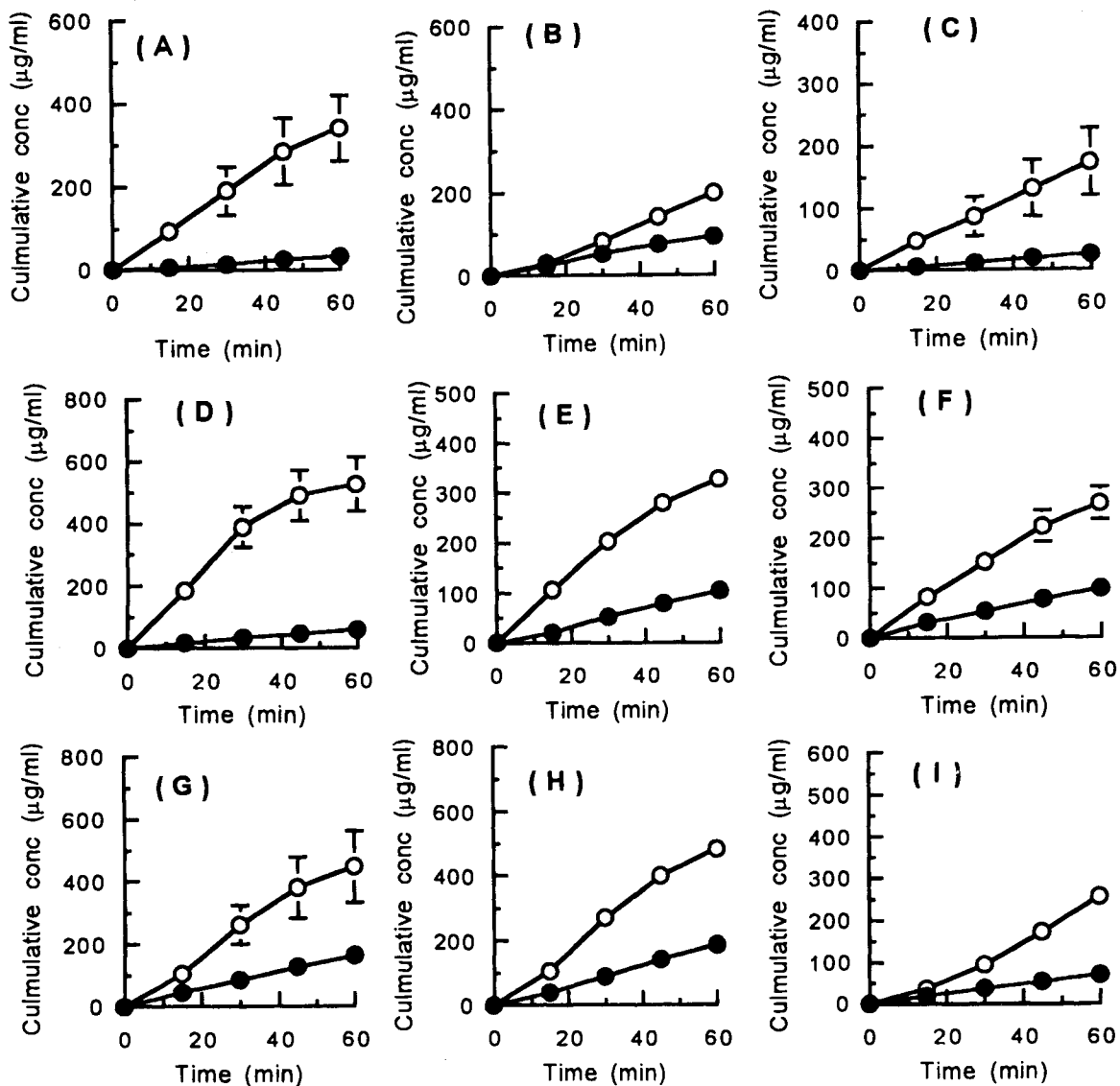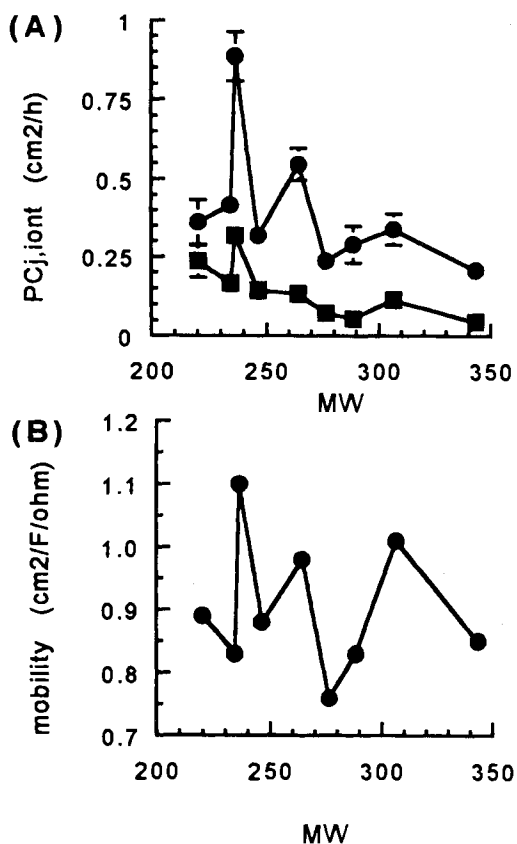
Fig. 1. The cumulative amount penetrated versus time profile for (A) bupivacaine, (B) butacaine, (C) cinchocaine, (D) etidocaine, (E) lidocaine, (F) mepivacaine, (G) prilocaine, (H) procaine and (I) tetracaine. Steady state fluxes were estimated from the linear portion of each profile. Key: (●) is donor pH at 4.5 and receptor pH at 4.5 and (○) is donor pH at 4.5 and receptor pH at 7.4 (mean ± s.e. n = 3).

Table III. Flux and $PC_{j,iont}$ of Local Anesthetics Studied (mean ± s.e., n = 3)

Local anesthetics	Receptor at pH 4.5		Receptor at pH 7.4	
	Flux (μmol/cm^2/h)	$PC_{j,iont}$ (cm/h)	Flux (μmol/cm^2/h)	$PC_{j,iont}$ (cm/h)
Bupivacaine	0.55 ± 0.01	0.055	2.88 ± 0.59	0.288
Butacaine	1.14 ± 0.14	0.114	3.77 ± 0.50	0.377
Cinchocaine	0.45 ± 0.02	0.045	2.06 ± 0.26	0.206
Etidocaine	0.72 ± 0.12	0.072	2.35 ± 0.29	0.235
Lidocaine	1.65 ± 0.13	0.165	4.15 ± 0.31	0.415
Mepivacaine	1.43 ± 0.17	0.143	3.17 ± 0.44	0.317
Prilocaine	2.35 ± 0.51	0.235	3.61 ± 0.71	0.361
Procaine	3.17 ± 0.16	0.317	8.84 ± 0.78	0.884
Tetracaine	1.33 ± 0.05	0.133	5.45 ± 0.51	0.545

(A)

(B)

MW

Fig. 2. (A) The relationship between $PC_{j,iont}$ of the local anesthetics with respect to MW (mean ± s.e. $n = 3$). Key: (◆) is donor pH at 4.5 and receptor pH at 4.5 and (●) is donor pH at 4.5 and receptor pH at 7.4. (B) The relationship between ionic mobility and MW of local anesthetics.

$$\log PC_{j,iont} =$$

$$4.16 - 0.0059 \ MW + 2.13 \log \text{ionic mobility} \qquad (15)$$

$$(r^2 = 0.96, n = 9)$$

for donor at pH 4.5 and receptor at pH 4.5 and

$$\log PC_{j,iont} =$$

$$3.45 - 0.0027 \ MW + 2.02 \log \text{ionic mobility} \qquad (16)$$

$$(r^2 = 0.82, n = 9)$$

for donor at pH 4.5 and receptor at pH 7.4. There was minimal covariance ($<1\%$) between MW and mobility in these regressions. The corresponding equations using MV rather than MW are:

$$\log PC_{j,iont} =$$

$$3.41 - 0.007 \ MV + 1.86 \log \text{ionic mobility} \qquad (17)$$

$$(r^2 = 0.93, n = 9)$$

for donor pH 4.5 and receptor pH 4.5 and

$$\log PC_{j,iont} =$$

$$3.11 - 0.003 \ MV + 1.90 \log \text{ionic mobility} \qquad (18)$$

$$(r^2 = 0.79, n = 9)$$

for donor pH 4.5 and receptor pH 7.4.

When a single pore size is assumed for the two pH conditions with different A terms in equation 6 corresponding to the two receptor pH's, poor regressions were obtained with $r^2 = 0.25$ for both MW and MV. The slope of 0.003 for both MW and MV at receptor pH 7.4 is almost identical to slopes obtained using this pH and a range of other solutes (1,5).

A higher free volume at a receptor pH of 4.5 is consistent with suppression of pore peptide ionization at its isoelectric point, the loss of the Debye layer and less ordering of water in the pore as a consequence. The lower intercept at pH 4.5 may be due to the loss of permselectivity, as discussed earlier, or simply the differences in solution conductivity between the solutions at pH 4.5 and 7.4.

The MW and MV at receptor pH 7.4 correspond to an average free volume of 161 and 144 (cm^3/mol) was deduced from the free volume model for MW and MV, respectively. From these free volumes, a corresponding r_j of about 4 Å and 3.9 Å, respectively was estimated. Yoshida & Roberts (3) noted that their average "cage" volume 155 cm^3/mol, based on a receptor pH of 7.4 corresponds to a solute of a radius of about 4 Å.

Figure 3 shows the resulting regressions of predicted log $PC_{j,iont}$ against observed log $PC_{j,iont}$. Through stepwise regression analysis, we attempted to determine whether the iontophoretic permeability coefficient ($PC_{j,iont}$) was related to other physical properties of the solute. We examined the combination of factors such as MW, pK_a, conductivity, MV and octanol-water partition coefficient in both normal and logarithmic forms of the free base to determine the best predictor of log $PC_{j,iont}$. From the results of this regression, it was found that the majority of the data (82.5% for receptor pH at 7.4 and 95.7% for receptor pH 4.5) is accounted for by the variables MW, MV and conductivity (or ionic mobility), as consistent with the regression equa-

iontophoretic flux. The findings were apparent at both pH 7.4 and pH 4.5 for the donor solution. A pH of 4.5 is at least 2 units below the local anesthetic pK_a, ensuring $>99\%$ of the local anesthetic is in an ionized form. It is not certain why the iontophoretic flux with the receptor at pH 4.5 is lower than when compared to the receptor pH 7.4 (Fig. 2), but one possible explanation is that at pH 4.5 there is a suppression of ionizable groups in the pore, leading to a decrease in the permselectivity factor Ω. This change in Ω will facilitate Cl$^-$ transport from the receptor at the expense of cations from the donor, especially the local anesthetics. This explanation is more likely than a change in receptor solution conductivity (equation 3), as this remained relatively constant at 16.4 mS for pH 7.4 and 14.3 mS for pH 4.5. The constant conductivity reflects the dominant effect of NaCl in the receptor solution on the overall conductivity. We now consider the determinant of local anesthetic transport using the ionic mobility-pore model assuming a free volume approach.

Ionic Mobility-Free Volume Pore Model

The relationships between log $PC_{j,iont}$ and other predictors defined by the free volume form of the ionic mobility-pore model (equation 6) were:
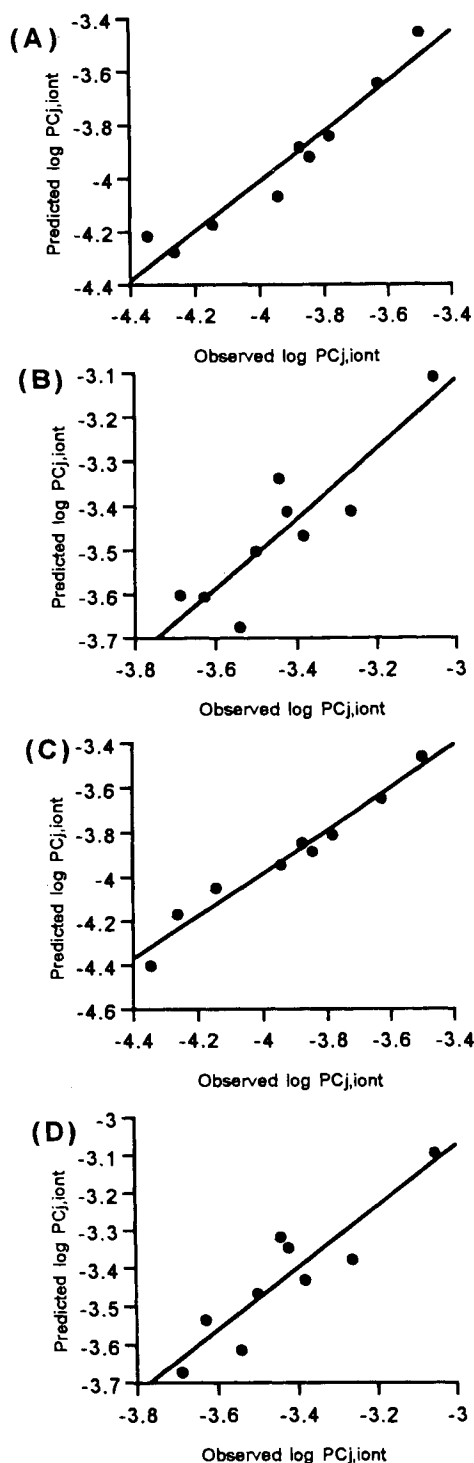
Fig. 3. Predicted and observed log $PC_{j,iont}$ for local anesthetics using the free volume form of the ionic mobility—pore model at (A) donor pH 4.5 and receptor pH 4.5 (MV and log ionic mobility), (B) donor pH 4.5 and receptor pH 7.4 (MV and log ionic mobility), (C) donor pH 4.5 and receptor pH 4.5 (MW and log ionic mobility), (D) donor pH 4.5 and receptor pH 7.4 (MW and log ionic mobility).

tion in equation 4 and expressed in equations 15 to 18. Thus it can be suggested that log $PC_{j,iont}$ is dependent on the logarithm of the ionic mobility and the size of the solute as defined by MW or MV.

The pK$_a$ was found to be a determinant of local anesthetic conductivity and consequently $PC_{j,iont}$ when conductivity was not a covariable. Equation 19 shows the expression for ionic mobility (deduced from conductivity using equation 14) in terms of its key determinants, pK$_a$ and MW:

log ionic mobility =

$$0.115\, pK_a - 0.001\, MW - 3.67\ (r^2 = 0.90, n = 9) \quad (19)$$

Equation 20 and 21 shows the expressions obtained for $PC_{j,iont}$ using pK$_a$ and MW and a determinant for receptor pHs of 4.5 and 7.4, respectively:

log $PC_{j,iont}$ =

$$0.19\, pK_a - 0.0079\, MW - 3.15\ (r^2 = 0.93, n = 9) \quad (20)$$

log $PC_{j,iont}$ =

$$0.23\, pK_a - 0.0046\, MW - 4.0\ (r^2 = 0.81, n = 9) \quad (21)$$

It is to be noted that the r^2 from these regressions are similar to those using ionic mobility and MW as determinants of $PC_{j,iont}$ (equations 15 and 16).

Given that earlier work from our group had used both solute conductivity and free volume as determinants of $PC_{j,iont}$ in separate studies, the potential improvement in r^2 from multiple regression relative to the limited single determinant regressions were compared. When solute ion mobility was assumed to be a sole predictor of log $PC_{j,iont}$, the regressions accounted for 51.7% and 28.3% of the data for donor pH 4.5, receptor pH 7.4 and donor pH 4.5, receptor pH 4.5, respectively. The corresponding % data obtained when MW alone was used as predictor of log $PC_{j,iont}$ were 33.4% and 71.3%. pKa as a sole predictor of log ionic mobility accounted for 60% of the data. This analysis confirms that both ionic mobility and size are determinants of $PC_{j,iont}$.

Ionic Mobility-Pore Restriction Model

In using the pore restriction form of the model, the assumption is made that homogeneity exists in pores, that is, they are uniform cylinders. However, Pikal (6) have shown evidence of heterogenous pore systems, in which factors such as tortuosity and different pore sizes are taken into consideration. Regressions with a large covariance between parameters was found when equation 3 was used in nonlinear regressions for a given set of pH conditions. However, the ionic mobility-pore model based on the pore restriction model (equations 3 and 8), and a single pore size for the two receptor pH's provided a good description of the observed local anesthetic data for both receptor pH at 7.4 and 4.5, estimating the pore radii to be 5.80 $\pm$ 0.49 Å (mean $\pm$ s.d., $n = 18$, $r^2 = 0.70$) and 5.50 $\pm$ 0.37 ($n = 18$, $r^2 = 0.69$) for MW and MV, respectively.

Comparison of Pore Radii Estimates

The pore size estimated in this study is similar to the pore size of 8 Å estimated independently by Yoshida & Roberts (3). Other pore size estimates in literature are 30 Å estimated by Yoshida & Roberts (5), 25 Å by Dinh et al. (12) and 20 Å by Li et al. (13) in human skin and 18 Å in hairless mouse skin by Ruddy & Hadzija (14).

The free volume model, in this study, provides a lower estimate of the pore size compared to the ionic mobility—pore model. This difference is expected because the free volume model is based on the movement or "jumping" of solute into an adjacent hole, whereas the ionic mobility—pore is based upon pore-restriction at both entry to pore and within the pore itself (3). The pore-restriction form of the model gives an absolute size limitation, but the free volume provides an estimate of the average free volume which is a measure of the size of the hole into which a solute, with an equal or smaller molecular size, can readily enter (3). The free volume model also suggests a difference in effective pore size at the two receptor pH conditions used.

The accuracy of pore radii estimated from the pore-restriction form of the model depends on an extensive range of r_j. In this series of local anesthetics used, because of the small range of r_j size, the accuracy of the estimation of r_p in this study is limited.

Effect of Charge on Solute and Membrane

A more accurate estimate of the actual pore size may be estimated if the effect of charge or the Debye layer is taken into account. From equation 11, the effect of the charge increases the size of the solute by the size of the Debye layer and decrease the pore radius by the Debye layer. The Debye layer, in our study was calculated to be 2.3 Å for the receptor solution with 147 mM NaCl and 3.9 Å for a donor solution containing 50 mM HEPES (equation 12). The relative effect of the donor and receptor solutions on the electrolyte composition in the pore is unknown. The predicted Debye layer effects when taken into consideration yield pore sizes of 7.80 ± 0.47 Å to 9.4 ± 0.47 Å ($n = 18$, $r^2 = 0.67$) and 7.50 ± 0.37 Å to 9.10 ± 0.37 Å ($n = 18$, $r^2 = 0.68$) for radii based on MW and MV, respectively. These estimates of pore size are very similar to that by Yoshida & Roberts (3). In this work, the effect of charge may be a more accurate representation of pore size due to the nature of the local anesthetics at donor pH 4.5. The different pH's used in the receptor phase will provide a pH gradient (donor pH 4.5 and receptor pH at 4.5 and 7.4) which will have an effect on the Debye layer and hence pore size.

Molecular Geometry of Solute

In estimating the pore radii, we assumed that the structure of the solutes were spherical in nature. In reality, the solutes are nonspherical with lower r_j and higher fluxes (4). The radii of solutes used in the analysis were estimated using MV calculated using the method of Yalkowsky & Zografi (15), which is a calculation based on the addition of partial atomic values. We also used other estimations of solute radii (16) (Table IV). There were no significant difference (2 way ANOVA) between each method of estimation of r_j.

Mobility of Iontophoresed Solute

As shown in equations 1 and 2, solute ionic mobility is a major determinant of iontophoretic transport. The ionic mobility of solutes are dependent on several factors, including interactions between the ions themselves, interactions between the ions and solvent molecules, size of the solute itself, and polarity of the solvent (17), polarity of the solute, solvation of the solute, presence of hydrogen bonding, viscosity of the solvent and temperature. Table V shows that the ionic mobility of local anesthetics are relatively independent of concentration, despite the 10-fold range in concentrations used.

One of the short comings of using conductivity measurements to calculate ionic mobilities is that these measurements reflects on the conductivity of the whole solution, that is, contributions of the cation as well as the anion. Apart from conductivity measurements, other methods of measuring ionic mobility include the ionic mobility spectroscopy (IMS) - gas chromatography, polarography, chronopotentiometry, isotachophoretic measurements (18) and free solution capillary electrophoresis (19), which are more direct methods of determining ionic mobilities of solutes, therefore overcoming these short comings. Polásek et al. (18), found that the mobility of a range of different local anesthetics (MW 271.8–433.9) determined by mobility of isotachophoresis was related to MW, with a r^2 of 0.59. The ionic mobility for the present range of local anesthetics are poorly related to MW ($r^2 = 0.22$) perhaps due to the smaller MW range used (220.3–343.4). However, local anesthetic ionic mobilities determined by conductivity (Table V) were found to be in the same order of magnitude, although slightly higher than

Table IV. Molal Volume (MV), MW and Estimated r_j of Solutes Studied

Local anesthetics	Partial molal volume (cm³/mol)[a]	Estimated r_j (Å) from MV	MW (Da)	Estimated r_j (Å) from MW	Molal volume (cm³/mol)[b]	Estimated r_j (Å) from molal volume	Molal volume including dead space (cm³/mol)[b]	r_j (estimated from molal volume including dead space) (Å)
Bupivacaine	273.5	4.8	288.4	4.9	292.4	4.9	397.3	5.4
Butacaine	285.2	4.8	306.4	5.0	293.0	4.9	398.5	5.4
Cinchocaine	276.5	4.8	343.4	5.1	277.9	4.8	377.9	5.3
Etidocaine	263.6	4.7	276.4	4.8	270.6	4.8	368.8	5.3
Lidocaine	215.3	4.4	234.3	4.5	238.2	4.6	324.0	5.0
Mepivacaine	225.2	4.5	246.3	4.6	243.8	4.6	331.6	5.1
Prilocaine	199.2	4.3	220.3	4.4	222.0	4.5	301.9	4.9
Procaine	204.7	4.3	236.3	4.5	228.2	4.5	310.4	4.9
Tetracaine	236.9	4.6	264.3	4.7	260.6	4.7	354.4	5.2

[a] Estimated from ref. 15.
[b] Estimated from ref. 16.

Table V. Intrinsic Conductivity and Mobility of the Local Anesthetics Studied at 1 mM and 10 mM

Local anesthetic	Concentration (mM)	Intrinsic conductivity (μS/cm)	Mobility (cm^2/ohm/F)
Prilocaine	1	85.7	0.89
	10	843	0.87
Lidocaine	1	79.9	0.83
	10	773	0.80
Procaine	1	106.3	1.10
	10	1143	1.18
Mepivacaine	1	84.7	0.88
	10	770	0.80
Tetracaine	1	94.6	0.98
	10	900	0.93
Butacaine	1	97.6	1.01
	10	1060	1.09
Etidocaine	1	73.5	0.76
	10	780	0.81
Bupivacaine	1	80.4	0.83
	10	740	0.77
Cinchocaine	1	81.8	0.85
	10	818	0.85

Note: Intrinsic conductivity measured in distilled deionized water at 25°C.

reported in the isotachophoretic experiments (18). Iontophoretic flux is also a function of the presence of drug ions.

This work has also shown that solute conductivity (and hence, ionic mobility (equation 14)) are significant determinants of local anesthetic $PC_{j,iont}$. The importance of conductivity as a determinant of solute transport has previously been recognised by Yoshida & Roberts (20,21) and Gangarosa et al. (22). Kamath & Gangarosa (23) had examined the relationship of various solutes and their iontophoretic transport and suggested that the transport of these solutes correlated with the pK_a on the basis that pK_a is a predictor of both their conductivity and ionized state. The present analysis also found that local anesthetic pK_a (Table II) was a determinant of their conductivities ($r^2 = 0.60$). When MW is added as a codeterminant of log ionic mobility, the percent of data explained is 90% (equation 19). pK_a was also found to be a determinant of log $PC_{j,iont}$ when used instead of conductivity as a determinant. Equation 20 suggests that the local anesthetic pK_a and MW account for 80–90% of log $PC_{j,iont}$, confirming the assertions of Kamath & Gangarosa (23) that solute pK_a is a key determinant of $PC_{j,iont}$. The present work suggests that both pK_a and MW are determinants of $PC_{j,iont}$.

Kamath & Gangarosa (23) also commented that because of the competition of hydronium ions at pH 5 with local anesthetic migration, the conductive state of all ions in the donor solution must be considered. Our studies were conducted at pH 4.5 so that all local anesthetics would be ionized and meaningful comparisons possible. A key prerequisite in such a comparison is a similar conductivity for the solution used. The conductivities of the donor solutions used ranged from 740 to 1,143 μSiemens/cm. Gangarosa et al. (22) also reported that the specific conductivity of lidocaine decreased as the solution pH increased from 5.36 to 6.89. In the present work, the conductivi-

ties of local anesthetics at 10 mM were 10 to 30% higher at pH 4.5 than at 7.4.

Interaction of Local Anesthetics with Pore Membranes

According to equations 3 and 5, the iontophoretic transport of ionized solutes also depends on the interaction with the membrane wall. This interaction includes (i) the partitioning of unionized components of solutes into pore membrane and (ii) the sorption of lipophilic cations onto the pore membrane surface on $PC_{j,iont}$ (4). An analysis of the iontophoretic transport of partially ionized solutes (24) with a defined interfacial transfer rate of unionized solutes accounted for the nonlinear $PC_{j,iont}$ versus fu_j relationships (4). Given that $fu_j = 0$ in this study, solute-pore interaction effects should be limited to the sorption kinetics of the local anesthetics as lipophilic cations, represented by θ_{ji} (equation 3). Guy and colleagues (25,26) have suggested that lipophilic cations interact with the skin by (i) "anchoring" the lipophilic part of the solute into the membrane and (ii) electrostatic interaction between the positive charge of the solute and the negative charge of the skin. These interactions have been shown to reduce convective flow. In the present work, a range of local anesthetics with varying lipophilicity was used. It may be anticipated that θ_{ji} is related to the apparent octanol-water partition coefficient (P_{app}) at pH 7.4. Non-significant regressions were found between $PC_{j,iont}$ and P_{app} (Table II) for the local anesthetics. It is possible that the interaction between the ionized local anesthetic and the pore membrane is similar for all local anesthetics and is significant, i.e., $\theta_{ji} > 0$. Accordingly, the observed $PC_{j,iont}$ may be less than the theoretical $PC_{j,iont}$ deduced ignoring this interaction by a factor of $1 + \theta_{ji}$.

Electroosmotic Flow

From equation 1, the contribution of electroosmotic flow to the total iontophoretic flux can be estimated by examining $v_m(1 - \sigma_j)$. Electroosmotic flow has been shown to move from the anode to the cathode compartment due to permselectivity of the skin (27). The role of convective transport during iontophoresis was discussed previously (4). In this work, the water flow, calculated from tritiated water flow, was 0.008 ± 0.0016 cm/h (mean $\pm$ s.e., $n = 18$, $r^2 = 0.99$). There were no significant difference observed in the water flux between the compounds and at the different receptor pH's. The $PC_{j,iont}$ for local anesthetics (Table III) is at least an order of magnitude more, confirming that convective flux ($1 - \sigma_j)v_m$ (equation 3) associated with water flow v_m was not a major determinant of local anesthetic flux in this study.

Other Factors

This work was limited to cations and the influence of permselectivity (equations 1 and 2) was studied only in the two cases of the pore peptides being either ionized at pH 7.4 or near their isoelectric points (pH 4.5). According to equations 2, $PC_{j,iont}$ is also proportional to the total current. Several studies (1,5,28) have demonstrated this proportionality.

Preferred Local Anesthetic for Iontophoresis

The present work suggests that the local anesthetic iontophoretic fluxes vary four fold with the greatest flux being appar-

ent for one of the smaller and least efficacious local anesthetics, procaine (Tables II and III). The similar order of magnitude suggests that clinical efficacy and experience may be the key determinant in the choice of local anesthetic for iontophoresis. The lag times for each of the local anesthetics for donor pH 4.5 and receptor 7.4 were similar.

CONCLUSIONS

This work sought to validate an ionic mobility—pore model developed earlier using the iontophoretic transport relationships for a range of local anesthetics. The iontophoresis for a range of local anesthetics was estimated using an identical contact current strength donor solution composition and anodal iontophoresis. The predictors of iontophoretic permeability coefficient ($PC_{j,iont}$) are ionic mobility, the conductivity of both the donor and receptor ions (including extraneous ions), total current density and permselectivity of the membrane. The free-volume mobility—pore model predictors of logarithm of iontophoretic permeability coefficient (log $PC_{j,iont}$) were confirmed to be solute mobility and MW. Local anesthetic flux into receptor chambers at pH 7.4 was found to be higher than those at pH 4.5. Analysis of local anesthetic iontophoretic permeability data with the model resulted in an average pore radius of about 10 Å.

ACKNOWLEDGMENTS

REFERENCES

1. M. S. Roberts, J. Singh, N. Yoshida, and K. I. Currie. Iontophoretic transport of selected solutes through human epidermis. In R. C. Scott, J. Hadgraft and R. Guy (eds.), *Prediction of Percutaneous Absorption*; IBC Technical Services Ltd, London, 1990, pp. 231–241.
2. J. B. Phipps and J. R. Gyory. Transdermal ion migration. *Adv. Drug Del. Rev.* **9**: 137–176 (1992).
3. N. H. Yoshida and M. S. Roberts. Solute molecular size and transdermal iontophoresis across excised human skin. *J. Contr. Rel.* **25**:177–195 (1993).
4. M. S. Roberts, P. M. Lai, and Y. G. Anissimov. Epidermal iontophoresis: I. Development of the ionic mobility-pore model. *Pharm. Res.* **15**:1569–1578 (1998).
5. N. H. Yoshida and M. S. Roberts. Structure-transport relations in transdermal iontophoresis. *Adv. Drug Del. Rev.* **9**:239–264 (1992).
6. M. J. Pikal. The role of electroosmotic flow in transdermal iontophoresis. *Adv. Drug Del. Rev.* **9**:201–237 (1992).
7. W. M. Deen. Hindered transport of large molecules in liquid-filled pores. *AIChE J.* **33**:1409–1425 (1987).
8. W. D. Munch, L. P. Zestar, and J. L. Anderson. Rejection of polyelectrolytes from microporous membranes. *J. Membr. Sci.* **5**:77–102 (1979).
9. A. Martin, J. Swarbrick, and A. Cammarata. *Physical Pharmacy* 3rd ed., Lea & Febiger, Philadelphia, 1983.
10. A. M. Kligman and E. Christophers. Preparation of isolated sheets

11. of human stratum corneum. *Arth. Dermatol.* **88**:702–705 (1963).
11. R. D. Purves. Accuracy of numerical inversion of Laplace transforms for pharmacokinetic parameter estimation. *J. Pharm. Sci.* **84**:71–74 (1995).
12. S. Dinh, C. W. Luo, and B. Berner. Upper and lower limits of human skin electrical resistance in iontophoresis. *AIChE J.* **39**:2011–2018 (1993).
13. S. K. Li, A. H. Ghanem, K. D. Peck, and W. I. Higuchi. Iontophoretic Transport across a synthetic membrane and human epidermal membrane: a study of the effects of permeant charge. *J. Pharm. Sci.* **86**:680–689, 1997.
14. S. B. Ruddy and B. A. Hadzija. Iontophoretic permeability of polyethylene glycols through hairless rat skin: application of hydrodynamic theory for hindered transport through liquid-filled pores. *Drug Des. Discovery* **8**:207–224 (1992).
15. S. H. Yalkowsky and G. Zografi. Calculation of partial molal volume in micellar systems. *J. Pharm. Sci.* **61**:793–795 (1972).
16. J. Vinter, A. Davis, M. Saunders, and N. Van Openbosch. Computation and Structure Manipulation In Chemistry (COSMIC). SKF & Wellcome 1978–1986.
17. H. Sjöberg, K. Karami, P. Beronius, and L. O. Sundelöf. Ionization conditions for iontophoretic drug delivery. A revised pK_a of lidocaine hydrochloride in aqueous solution at 25°C established by precision conductometry. *Int. J. Pharm.* **141**:63–70 (1996).
18. M. Polásek, B. Gas, T. Hirokawa, and J. Vacik. Determination of limiting ionic mobilities and dissociation constants of some local anaesthetics. *J. Chromatograph.* **596**:265–270 (1992).
19. M. C. Heit, A. McFarland, R. Bock, and J. E. Riviere. Isoelectric focusing and capillary zone electrophoretic studies using luteinizing hormone releasing hormone and its analog. *J. Pharm Sci.* **83**:654–656 (1994).
20. N. H. Yoshida and M. S. Roberts. Role of conductivity in iontophoresis, 2. Anodal iontophoretic transport of phenylethylamine and sodium across excised human skin. *J. Pharm. Sci.* **83**:344–350 (1994).
21. N. H. Yoshida and M. S. Roberts. Prediction of cathodal iontophoretic transport of various anions across excised skin from different vehicles using conductivity measurements. *J. Pharm. Pharmacol.* **47**:883–890 (1995).
22. L. P. Gangarosa, N. H. Park, B. C. Fong, D. F. Scott, and J. M. Hill. Conductivity of drugs used for iontophoresis. *J. Pharm. Sci.* **67**:1439–1443 (1978).
23. S. S. Kamath and L. P. Gangarosa, Sr. Electrophoretic evaluation of the mobility of drugs suitable for iontophoresis. *Meth. Find. Exp. Clin. Pharmacol.* **17**:227–232 (1995).
24. O. Siddiqui, M. S. Roberts, and A. E. Polack. Iontophoretic transport of weak electrolytes through the excised human stratum corneum. *J. Pharm. Pharmacol.* **41**:430–432 (1989).
25. J. Hirvonen and R. H. Guy. Iontophoretic delivery across the skin: electroosmosis and its modulation by drug substances. *Pharm. Res.* **14**:1258–1263 (1997).
26. M. B. Delgado-Charro and R. H. Guy. Characterization of convective solvent flow during iontophoresis. *Pharm. Res.* **11**:929–935 (1994).
27. M. J. Pikal and S. Shah. Transport mechanisms in iontophoretisis. II. Electroosmotic flow and transference number measurements for hairless mouse skin. *Pharm. Res.* **7**:213–221 (1990).
28. P. M. Lai and M. S. Roberts. Iontophoresis. In M. S. Roberts and K. Walters (eds), *Dermatological Formulations and Toxicology*, Marcel Dekker. In press.
29. G. T. Tucker and L. E. Mather. Properties, absorption, and disposition of local anesthetic agents. In M. J. Cousins and P. O. Bridenbaugh (eds), *Neural Blockade in Clinical Anesthesia and Management of Pain* 2nd ed, J.B. Lippincott Co., Philadelphia 1988 Chap. 2.
30. W. C. Bowman and M. J. Rand. *Textbook of Pharmacology* 2nd Ed., Blackwell Scientific Publications, Oxford 1980 p. 40.4.